DOI: 10.1002/chem.200701111

Supramolecular Gels Formed by Amphiphilic Low-Molecular-Weight Gelators of N^{α},N^{ε}-Diacyl-L-Lysine Derivatives

M. Suzuki,* M. Yumoto, H. Shirai, and K. Hanabusa[a]

Abstract: Simple L-lysine derivatives, N^{α}-hexanoyl-N^{ε}-lauroyl-L-lysine (**1**), its alkali metal salts (**2**–**4**), and two-component compounds that consist of **1** with **2** to **4**, were synthesized and their hydrogelation and organogelation properties were studied. Addition of hydrochloric acid to an aqueous solution of the alkali metal salt at room temperature produced a translucent hydrogel. This hydrogelation occurred as a result of a change in nanostructure from micelle-like aggregates to nanofibers, which was induced by partial protonation of the carboxylate to form a carboxylic acid. On the other hand, two-component low-molecular-weight gelators exhibited amphiphilic gelation behavior and functioned as not only hydrogelators, but also as organogelators. FTIR studies revealed that lateral ionic interactions between the carboxylate, alkali metal cation, carboxylic acid, and protons, in addition to hydrogen-bonding and van der Waals interactions play a very important role in hydrogelation. Furthermore, it was found that the water-insoluble carboxylic acid compound underwent a precipitation–dissolution transition with a thermally reversible sol–gel transition in the two-component gelator systems.

Keywords: gels · lysine · nanostructures · sol–gel processes · supramolecular chemistry

Introduction

When organic compounds are dissolved in a solvent and the solution is cooled, most organic compounds crystallize (> saturated concentration) or keep dissolving (dilute solution). Some compounds form a supramolecular gel and are known as low-molecular-weight gelators; more specifically, they are known as organogelators for organic solvents and oils and hydrogelators for aqueous solutions.[1–3] A number of low-molecular-weight gelators have been found, and their gelation abilities and mechanisms have been reported.[1–6] Most supramolecular gels are composed of long nanofibers (supramolecular polymers) that are self-assembled as a result of the usual array of noncovalent forces, such as hydrogen bonding, van der Waals, π-stacking, coordination, electrostatic, and charge-transfer interactions. Noncovalent crosslinks and physical entanglements among the supramolecular polymers create a three-dimensional network with solvent molecules immobilized in the nanospaces.

Recently, low-molecular-weight gelators have been of interest not only for their gelation behavior, but also because they form nanostructures in the supramolecular gels, such as nanofibers, nanoribbons, nanosheets, nanoparticles, helical, and bundle structures. The nanostructure can be controlled by choosing suitable gelators and solvents. Nanostructures have been used as an organic template for the fabrication of mesoporous polymer materials[7] and the nanoscale design of inorganic materials.[8,9] Sol–gel polymerization of metal alkoxides (Si, Ti, Ta, V, Ge, etc.) in solvents that contain gelators produces nanostructured metal oxides, such as nanotubes, helical nanofibers, and bundled nanofibers.[8] The reduction of metal ions (Ag, Au, etc.) in the presence of gelators forms an array of metal nanoparticles.[9] In addition, gelators are used as a scaffold for the mineralization of hydroxyapatite[10] and as a matrix for the growth of calcite crystals.[11] Other applications include their use as gel electrolytes,[12] liquid crystals,[13] photochemicals,[14] pharmaceuticals,[15] drug and gene delivery,[16] and so on.[17]

We have focused on the gelation behavior and self-assembling properties of organogelators and have developed some hydrogelators based on L-lysine according to a concept based on the conversion of organogelators into hydrogelators.[5a,18,19] The strategy involves introducing charged or un-

[a] Dr. M. Suzuki, M. Yumoto, Prof. Dr. H. Shirai, Prof. Dr. K. Hanabusa
Graduate School of Science and Technology
Shinshu University
Ueda, Nagano 386-8567 (Japan)
Fax: (+81) 268-21-5608
E-mail: msuzuki@shinshu-u.ac.jp

Supporting information for this article is available on the WWW under http://www.chemeurj.org/ or from the author.

charged hydrophilic groups into organogelators. L-Lysine compounds with a positively charged pyridinium or uncharged aldonamide functionality are excellent hydrogelators, whereas the negatively charged L-lysine derivatives are not necessarily good hydrogelators. To improve the hydrogelation ability of the negatively charged hydrogelators, many derivatives have been synthesized. Carboxylic acid derivative **1** is water-insoluble, whereas its alkali metal salts (**2**–**4**) are readily soluble in water. These compounds have no hydrogelation abilities by themselves. Very interestingly, it was found that the compounds prepared from **1** to **4** had good hydrogelation abilities. In addition, these compounds exhibited pH-triggered hydrogelation and amphiphilic gelation, thus forming not only hydrogels, but also organogels. Herein, we describe the simple preparation of two-component amphiphilic gelators based on L-lysine, their gelation properties in aqueous solutions and organic solvents, and pH-triggered hydrogelation.

Results and Discussion

Acid-triggered hydrogelation: When a specific amount of 0.1 M aqueous HCl was added to an aqueous solution of **2** (10 mg mL^{-1}) at 25 °C with vigorous stirring, the aqueous solution changed to a translucent hydrogel that was stable to inversion. The reaction conditions are listed in Table 1. Hydrogelation occurs on adding 0.134 to 0.356 mL (samples C–H) of aqueous HCl. The addition of 0.044 and 0.089 mL of 0.1 M HCl produces a viscous aqueous solution, whereas the opaque hydrogels that contain a water-insoluble white precipitate are obtained by adding 0.267, 0.312, and 0.356 mL HCl (samples F–H). The translucent hydrogels are obtained by adding 0.134 to 0.223 mL HCl (samples C–E). Because the addition of aqueous HCl to the aqueous solution of **2** partly forms **1**, hydrogelation will be induced by a mixture of **2** and **1**. On the other hand, the hydrogels formed changed into an isotropic solution at 25 °C on stirring followed by the addition of a molar equivalent of aqueous NaOH with respect to the aqueous HCl previously added. The sol–gel transition is thus reversible by repeating the addition of aqueous HCl and aqueous NaOH above the minimum gel concentration (MGC).

Table 1. Reaction conditions for pH-triggered hydrogelation at 25 °C.[a]

Sample	H/Na[b]	H_2O [mL]	0.1 M HCl [mL]	Aspect[c]
A	1:9	1.956	0.044	VS
B	2:8	1.911	0.089	VS
C	3:7	1.866	0.134	TL gel
D	4:6	1.822	0.178	TL gel
E	5:5	1.777	0.223	TL gel
F	6:4	1.733	0.267	OP gel
G	7:3	1.688	0.312	OP gel
H	8:2	1.644	0.356	OP gel
I	9:1	1.600	0.400	PG

[a] [**3**] = 20 mg (4.46×10^{-2} mmol). [b] Ratios of H^+ and **3**. [c] Gels contain a white precipitate. TL: translucent, OP: opaque, VS: viscous solution, PG: partial gel.

Because the formation of supramolecular hydrogels involves the self-organization of gelators, a heating process needs to dissolve and disperse gelators into an aqueous solution. In the present system, however, note that hydrogelation occurs at room temperature.

Hydrogelation in two-component hydrogelators: Detailed studies were carried out by using two-component compounds **2e**, **3a**–**3i**, and **4e**. These compounds were prepared by partial neutralization of **1** with aqueous NaOH for **3a** to **3i**, aqueous LiOH for **2e**, and aqueous KOH for **4e**. The hydrogelation properties of these compounds are listed in Table 2. Compounds **3a** (**1**/**3** = 1:9) and **3i** (**1**/**3** = 9:1) had no hydrogelation ability, whereas **3b** to **3h** (**1**/**3** = 2:8–8:2) formed hydrogels. Compounds **3b** to **3e** (**1**/**3** = 2:8–5:5) completely dissolved in pure water during heating and then produced translucent hydrogels after standing at 25 °C for 6 h. In contrast, **3f** to **3h** (**1**/**3** = 6:4–8:2), which had an excess of **1** compared with **3**, were partly soluble in pure water and formed hydrogels that contained a water-insoluble white solid. These results are almost the same as those in Table 1. Therefore, acid-triggered hydrogelation is induced by the partial formation of **1**. The water-insoluble solid in **3f** to **3h** was identified by FTIR, ^{1}H NMR, and elemental analysis, and these data were consistent with those of **1**. This fact indicates that **1** and **3** form a water-soluble 1:1 complex. On the other hand, the hydrogelation ability was independent of the alkali metal ions and similar MGC values were observed for **2e**, **3e**, and **4e**. These hydrogelators also formed hydrogels in aqueous solutions that contain inorganic salts, such as saline, NaCl, and KCl.

Table 2. Hydrogelation properties of **1**–**4** at 25 °C.[a]

Gelators	H/M[b]	H_2O	Saline[d]	NaCl[e]	KCl[e]
1	10:0	ins	ins	ins	ins
2	0:10	Sol	sol	sol	sol
2e	5:5	GTL (7)	GTL (10)	GTL (7)	GTL (7)
3	10:0	Sol	sol	sol	sol
3a	1:9	PG	PG	PG	PG
3b	2:8	GTL (20)	GTL (17)	GTL (17)	GTL (20)
3c	3:7	GTL (9)	GTL (9)	GTL (7)	GTL (7)
3d	4:6	GTL (9)	GTL (8)	GTL (5)	GTL (7)
3e	5:5	GTL (8)	GTL (8)	GTL (5)	GTL (7)
3f	6:4	GO (8)[c]	GO (10)	GO (8)	GO (10)
3g	7:3	GO (8)[c]	GO (10)	GO (8)	GO (12)
3h	8:2	GO (15)[c]	GO (15)	GO (15)	GO (20)
3i	9:1	PG	PG	PG	PG
4	10:0	sol	sol	sol	sol
4e	5:5	GTL (7)	GTL (10)	GTL (7)	GTL (7)

[a] MGC [g L^{-1}] value given in parentheses. [b] Molecular ratios of **1** and its alkali metal salts. [c] Gels contain a white precipitate. [d] Saline contains NaCl (8.6 g L^{-1}, ≈0.147 M), KCl (0.3 g L^{-1}, ≈4.02×10^{-3} M), and $CaCl_2$ (0.33 g L^{-1}, ≈2.97×10^{-3} M). [e] [NaCl] = [KCl] = 0.1 M. GTL: translucent gel; GO: opaque gel; ins: insoluble; sol: solution; PG: partial gel.

Organogelation properties: These two-component compounds (**2e**–**4e**) have not only hydrogelation ability, but also organogelation ability, as listed in Table 3. For all compounds, they were insoluble in *n*-hexane and readily soluble in alcohols. Compared with **1**, its alkali metal salt compounds (**2**–**4**) have a better organogelation property, and two-component gelators (**2e**–**4e**) demonstrate similar properties. Compounds **2e** to **4e** can form organogels in esters, ketones, cyclic ethers, aromatic solvents, CCl_4, vegetable oils, and mineral oils. It is generally known that organogelation often depends on the balance between hydrophilicity and hydrophobicity of gelator molecules.[1–6] Because the two-component gelators (**2e**–**4e**) consist of hydrophobic compound **1** and hydrophilic compounds (**2**–**4**), their suitable hydrophobic–hydrophilic balances lead to a high organogelation ability; for example, although **2** to **4** have no gelation ability for vegetable oils, derivatives **2e** to **4e** gel them. In addition, compound **4e** showed a lower organogelation ability than **2e** and **3e**. Such different organogelation ability is exemplified by that of **4**. It is likely that **4** has a lower hydrophilicity than **2** and **3**.

Table 3. Organogelation properties of **1**–**4** and **2e**–**4e** at 25 °C[a]

Solvents	**1**	**2**	**3**	**4**	**2e**	**3e**	**4e**
n-hexane	ins	ins	ins	ins	ins	ins	ins
cyclohexane	PG	PG	PG	PG	PG	PG	PG
EtOH	sol	sol	sol	sol	sol	sol	sol
AcOEt	15	P	PG	ins	15	12	ins
acetone	45	ins	PG	ins	15	20	ins
cyclohexanone	S	3	10	3	3	25	5
dioxane	55	6	7	5	3	7	10
Ph−H	25	12	3	30	7	3	20
Ph−CH_3	PG	3	3	30	5	3	15
Ph−Cl	20	4	3	30	3	3	10
Ph−NO_2	3	8	5	7	10	7	10
DMSO	sol	25	sol	45	PG	sol	sol
$CHCl_3$	sol	30	sol	sol	sol	sol	25
CCl_4	3	15	30	25	10	30	PG
oleic acid	15	sol	sol	sol	40	20	40
linoleic acid	15	sol	sol	sol	40	20	40
diesel oil	PG	12	5	5	3	5	3
kerosene	PG	12	5	5	8	5	8

[a] Values denote MGC [$g L^{-1}$]. ins: insoluble, PG: partial gel, P: precipitate after dissolution, sol: solution at 30 $g L^{-1}$.

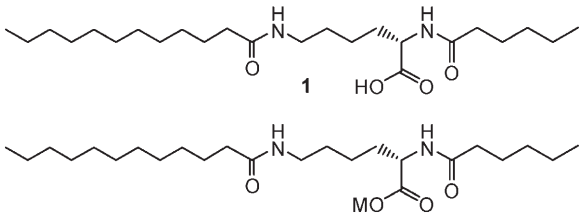

2e: **1**/**2** (5:5)
3a: **1**/**3** (1:9); **3b** **1**/**3** (2:8); **3c**: **1**/**3** (3:7); **3d**: **1**/**3** (4:6)
3e: **1**/**3** (5:5); **3f**: **1**/**3** (6:4); **3g**: **1**/**3** (7:3); **3h**: **1**/**3** (8:2)
3i: **1**/**3** (9:1)
4e: **1**/**4** (5:5)

TEM studies: It is known that a gelator molecule constructs nanoscale superstructures, such as nanofibers, nanoribbons, and nanosheets, in a supramolecular gel.[1] Figure 1 shows the transmission electron microscopy (TEM) images of dried gels prepared from a pure water gel, a saline gel, a 0.1 M aqueous NaCl gel, a benzene gel, a 1,4-dioxane gel, and a CCl_4 gel of **3e**. In all of the supramolecular gels, compound **3e** formed supramolecular nanofibers (10–40 nm in diameter) whose entanglements created a three-dimensional network. Similar images were observed for other gelators. Therefore, organogelation and hydrogelation occur by immobilizing solvents in the nanospaces in the three-dimensional networks.

On the other hand, the TEM images of **3** in pure water and a partial gel of pure water based on **3a** are shown in Figure 2. Compound **3** formed spherical micelles with a di-

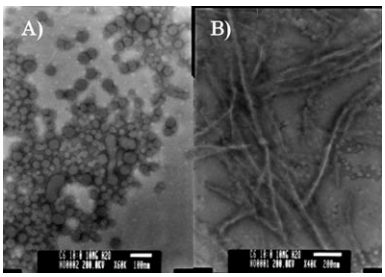

Figure 2. TEM images of dried samples prepared from A) a pure water solution of **3** and B) a partial gel of **3a**. Scale bar: 100 nm (in A) and 200 nm (in B).

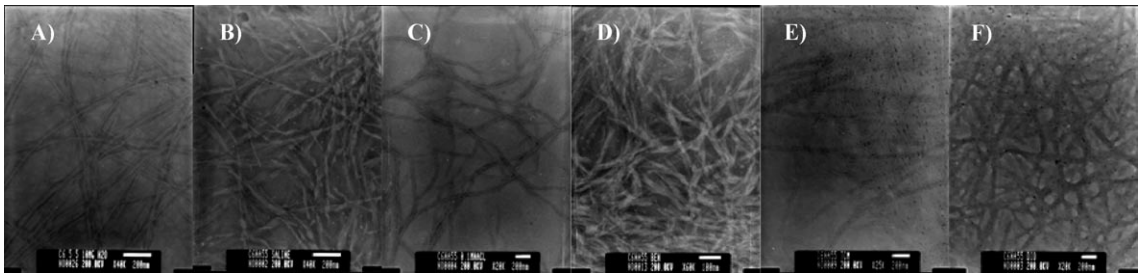

Figure 1. TEM images of dried samples prepared from A) pure water gel, B) saline gel, C) 0.1 M aqueous NaCl gel, D) benzene gel, E) CCl_4 gel, and F) 1,4-dioxane gel of **3e**. Scale bar: 200 nm (in A–C, E, F) and 100 nm (in D).

ameter of 30–100 nm that did not lead to hydrogelation. In contrast, the TEM image of **3a** showed that it formed spherical micelles (30–100 nm in diameter) and self-assembled nanofibers (30–80 nm in diameter). Considering the ratio of **1** and **3** (1:9) in **3a**, compound **1** and some of **3** form a complex and self-assemble into nanofibers, whereas excess **3a** forms the micelles. Note that the presence of a little **1** leads to the formation of nanofibers.

FTIR studies: The FTIR spectra of **1**, **3**, and **3a** to **3i** in the solid state revealed similar absorption bands at around $\tilde{\nu}=$ 1640 (amide I) and 1550 cm^{-1} (amide II), thus providing important data for the interaction between **1** and **3** at $\tilde{\nu}=$ 1740–1700 cm^{-1} that arises from the C=O stretching vibration of the carboxylic acid.[20] The absorption band of $\nu_{C=O}$ (CO_2H) appeared at 1734 cm^{-1} for **1**, but not for **3** because it does not have a carboxylic acid group. For two-component compounds **3f** to **3i**, the absorption band shifted to a lower wavenumber and a new peak at $\approx$1709 cm^{-1} was observed as the proportion of **3** increased. Compounds **3a** to **3e** showed one IR band at 1709 cm^{-1}. It is known that the IR spectrum of a dimerized carboxylic acid is observed at around $\tilde{\nu}=$1700–1710 cm^{-1}.[21] Considering the solubility of **3a** to **3f** in water, it indicates that **1** and **3** form a dimer between the carboxylic acid and the carboxylate mediated by a sodium ion and a proton; therefore, the hydrogelation ability arises from the formation of a water-soluble dimer. Moreover, dimer formation between **1** and **3** is independent of the countercations, and **2e** (Li^+) and **4e** (K^+) show the same hydrogelation abilities as **3e**.

It is generally known that a low-molecular-weight gelator forms self-assembled nanofibers in a supramolecular gel through hydrogen bonding and van der Waals (hydrophobic) interactions, which can be analyzed by NMR and FTIR spectroscopies, and X-ray analysis.[1–8] FTIR spectroscopy, in particular, is a powerful tool for structural analysis and has been extensively used to investigate organogelation because the IR spectrum of the gel state in addition to solution and solid states can be obtained. In many cases, however, the FTIR spectrum has only been roughly analyzed owing to the overlap of some IR peaks. In the present study, the recorded FTIR spectra were resolved by using a curve-fitting technique (JASCO FTIR Plus Series Curve Fitting version 2.00F). Figure 3 shows the FTIR spectra of **3** and **3a** (as solutions in D_2O) and **3b** to **3e** (as D_2O gels).[22] The FTIR spectra showed two (**3** and **3a**) or three (**3b**–**3e**) broad IR bands in D_2O at 1726, 1625 (or 1617), and 1587 cm^{-1}, arising from the stretching vibration of the carboxylic acid, amide I, and carboxylate groups, respectively. These bands were further resolved into five or six individual spectra by using the curve-fitting program. With respect to the ratio of band areas, the main IR bands are at 1625 and 1613 cm^{-1} ($\nu_{C=O}$, amide I) and 1587 cm^{-1} (ν_{C-O}, -COO^-) for **3** and **3a** as well as at 1726 cm^{-1} ($\nu_{C=O}$, -COOH), 1626 and 1609 to 1613 cm^{-1} ($\nu_{C=O}$, amide I) and 1586 cm^{-1} (ν_{C-O}, -COO^-) for **3b** to **3e**.[20,23] It is interesting that hydrogen-bonded amide I is resolved into two spectra, which indicates that these compounds have at least two hydrogen bonding modes in the micelles or nanofibers. This result is consistent with the fact that **3** and **3a** to **3e** have two amide bonds at the N^{α} and N^{ε} amide nitrogen atoms in the lysine. The amide group of the N^{ε} position is close to the hydrophobic alkyl group, whereas that of the N^{α} position neighbors the hydrophilic carboxylate group. In water (or hydrogel), the amide group of the N^{ε} position is located in a more hydrophobic area and undergoes a stronger hydrogen-bonding interaction than that of the N^{α} position; therefore, it is assumed that the IR peaks at around 1610 and 1626 cm^{-1} correspond to the amide groups of the N^{ε} position and N^{α} position, respectively.

As mentioned above, compounds **3b** to **3e** form the dimer between the carboxylic acid and the sodium carboxylate groups in the solid states, which is supported by the

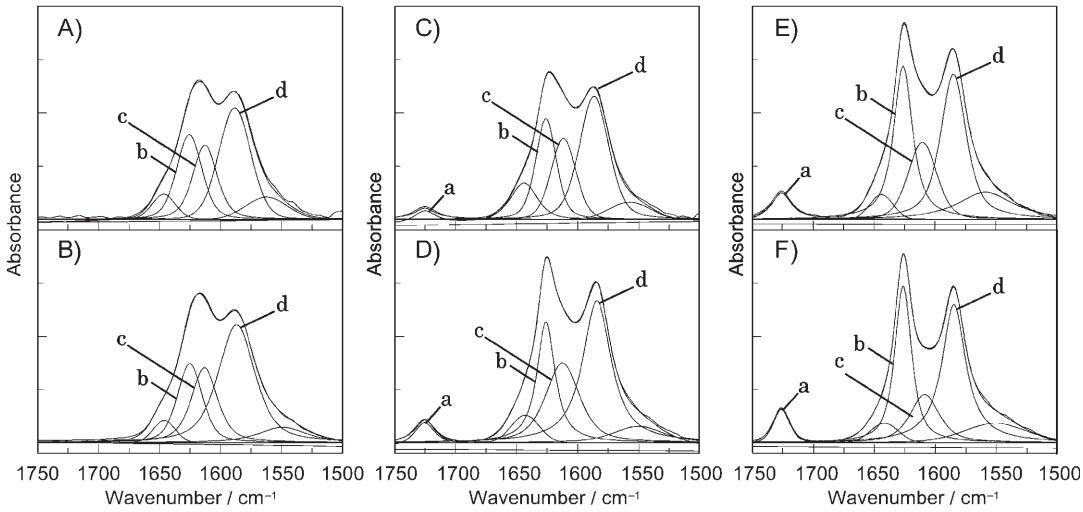

Figure 3. FTIR spectra and their curve-fitting results of **3** and **3a**–**3e** in D_2O (20 $g\,L^{-1}$). A) Solution of **3** in D_2O, B) solution of **3a** D_2O, C) D_2O gel of **3b**, D) D_2O gel of **3c**, E) D_2O gel of **3d**, F) D_2O gel of **3e**. IR peaks: a) $\nu_{C=O}$, -COOH, b) $\nu_{C=O}$, amide I, c) $\nu_{C=O}$, amide I, d) ν_{C-O}, -COO^-.

FTIR result. In the D_2O gel, however, the IR peak appears at 1725 cm^{-1}, which is similar to the lateral hydrogen-bonded carboxylic acid. This indicates that the carboxylic acid and carboxylate groups in **3b** to **3e** interact through a lateral hydrogen-bonding mode in the D_2O gel and it is likely that they have alternative interactions (···Na···OCO···H···O). Note that the structure of the gelators changes from the cyclic dimer to linear interactions.

In addition, the FTIR measurements also provide information on the alkyl groups. The absorption bands of the asymmetric (ν_{asym}) and symmetric (ν_{sym}) CH_2 stretching vibrations of **3e** were observed at 2921 and 2851 cm^{-1} in the D_2O gel. These bands appear at a lower frequency than those of free alkyl chains in $CHCl_3$ (2928 cm^{-1} (ν_{asym}, C–H) and 2856 cm^{-1} (ν_{sym}, C–H)). Such a low frequency shift indicates a strong interaction between the alkyl chains (hydrophobic interaction).[5a] Therefore, the driving forces for self-assembly into nanofibers (leading to the hydrogelation) are hydrogen bonding between the amide groups, interactions between the carboxylic acid and alkyl carboxylate, and hydrophobic interactions.

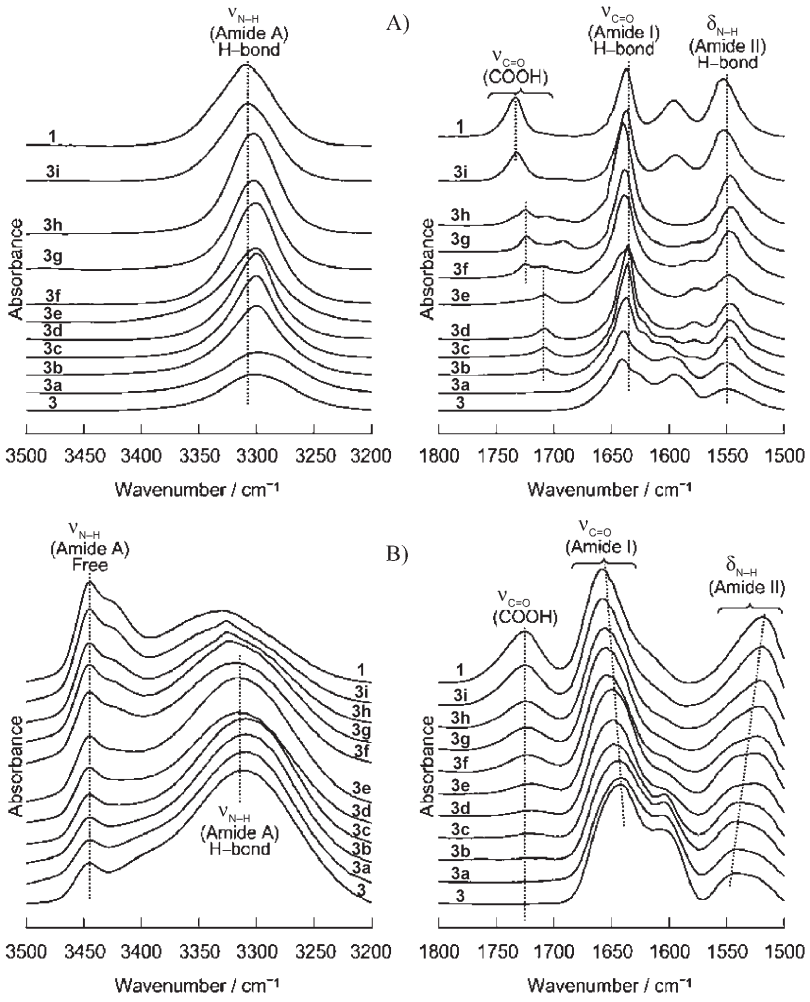

Figure 4. FTIR spectra of **1**, **3** and **3a**–**3i** in A) CCl_4 gels and B) $CHCl_3$ solution; [gelator] = 30 $g\,L^{-1}$.

The FTIR spectra of the CCl_4 gel based on **1**, **3** and **3a** to **3i** are shown in Figure 4A, and the resolved spectra and their data in the amide I region are shown in Figure S4 and Table S3 in the Supporting Information.[20] Typical IR bands were observed around 1635 cm^{-1} ($\nu_{C=O}$, amide I) and 1548 cm^{-1} (δ_{N-H}, amide II) in addition to 3300 cm^{-1} (ν_{N-H}, amide A), arising from hydrogen-bonded amide groups. This indicates hydrogen-bonding-induced organogelation similar to a common organogelator previously reported.[1] The curve-fitting results of the amide I region demonstrated that the IR band of amide I for these gelators was resolved into a number of bands (at around 1655, 1637, and 1620 cm^{-1}).[20] This result indicates that these gelators self-assemble into nanofibers through a number of hydrogen-bonding modes. Furthermore, the IR band of the C=O stretching vibration of the carboxylic acid at around 1740 to 1700 cm^{-1} was also interesting and almost the same as that of the solid state. For **1** and **3i**, the IR band was observed at 1733 cm^{-1}, whereas **3** and **3a** showed no bands between 1700 and 1800 cm^{-1}. Compounds **3f** to **3h** showed two peaks at 1724 and 1709 cm^{-1} and **3b** to **3e** had a peak at around 1708 cm^{-1}. These results indicate that **3b** to **3h** have a cyclic dimer structure with carboxylic acid and sodium carboxylate as a platform in the self-assembled nanofibers in the CCl_4 gels.[24] In the present case, both **1** and **3** have gelation ability for CCl_4 and can form self-assembled nanofibers. Except for **3e**, therefore, organogelation of **3a** to **3i** occurs through the formation of at least two self-assembled nanofibers; **3e** forms only the self-assembled nanofiber based on the cyclic dimer structure. Although it is not clear that **3** and **3e** in **3a** to **3d** or **1** and **3e** in **3f** to **3i** form a hybrid nanofiber or a separated one, compounds **3a** to **3d** that contain excess **3** form CCl_4 gels that consist of nanofibers of **3e** and **3**, and the gels of **3f** to **3i** are formed by nanofibers of **3e** and **1**. Such differences in interaction modes between carboxylic acid and carboxylate groups should cause the complex hydrogen-bonding modes between the amide groups.

Compounds **1** and **3f** to **3i** did not exhibit organogelation with $CHCl_3$ at 30 $g\,L^{-1}$, and the FTIR spectra showed typical bands for non-hydrogen-bonded amide groups at 3446 cm^{-1} (amide A), 1654 to 1658 cm^{-1} (amide I), and 1520 cm^{-1}

(amide II) in addition to 1725 cm^{-1} (Figure 4B). In contrast, the IR spectra of **3** and **3a** to **3e** shifted to a lower wavenumber with an increasing ratio of **3**, and those of **3**, **3a**, and **3b** appeared at 1642 cm^{-1} and 1543 cm^{-1}, which corresponded to the IR bands of hydrogen-bonded amide I and II. However, the IR band of amide A was also observed around 3446 cm^{-1} (free amide A). To elucidate these IR spectra, the broad IR band in the amide I region was resolved.[20] As expected, the IR spectra of **1** and **3f** to **3i** exhibited the IR band of non-hydrogen-bonded amide I (at 1658 cm^{-1}). In contrast, the IR spectra of **3** and **3a** to **3e** consisted of both hydrogen-bonded amide I bands (at 1625 and 1639 cm^{-1}) and a non-hydrogen-bonded amide I band (at 1658 cm^{-1}). This result indicates that part of the amide groups in **3** and **3a** to **3e** undergoes a hydrogen-bonding interaction in $CHCl_3$. The ^1H NMR spectroscopy study of **1**, **3**, and **3a** to **3i** in $CDCl_3$ demonstrates a low magnetic field shift and peak broadening of the proton in the amide group with the increasing ratio of **3**, and this is one piece of evidence for the presence of a hydrogen-bonding interaction.[20] The organogelation property for $CHCl_3$ of these gelators was examined at a high concentration. Compounds **1** and **3f** to **3i** have no gelation ability for $CHCl_3$ at 100 $g L^{-1}$, and **3c** to **3e** cannot form a $CHCl_3$ gel at 100 $g L^{-1}$, but produce a viscous solution. Compounds **3**, **3a**, and **3b** function as an organogelator for $CHCl_3$ at 80 $g L^{-1}$, although the MGC value is very high.

Gel strength and thermal stability of the hydrogels: The gel strength, which is an important factor in the wide application of gels, has been evaluated by measuring the elastic storage modulus G′ and loss modulus G″ at different gelator concentrations.[25] In our study, however, we evaluated the gel strength as the power that is required to sink a cylindrical bar (10 mm in diameter) 4 mm deep into the gel. Figure 5 shows the gel strength of hydrogels and saline gels based on **3c** and **3e** at the various concentrations. The gel strengths increased with the increasing concentrations of gelators. This is the reason why the hydrogelators create more closely three-dimensional networks at high concentrations.

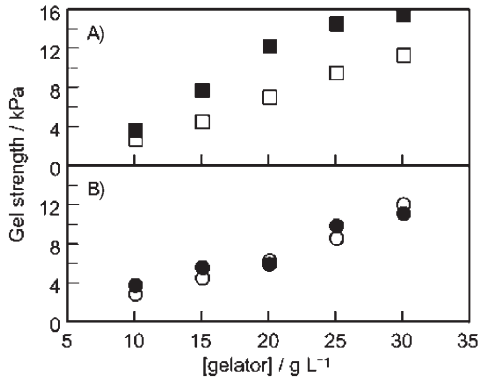

Figure 5. Gel strengths of hydrogels and saline gels based on **3c** and **3e** as a function of the gelator concentration. A) hydrogel (□) and saline gel (■) of **3c**; B) hydrogel (○) and saline gel (●) of **3e**.

The gel strength of a pure water gel of **3e** was almost the same as that of the saline gel. In contrast, the gel strength of **3c** gels was significantly affected by the ionic strength: the saline gel was more rigid than the hydrogel. The gel strength, which corresponds to the hardness of a gel, is chiefly dependent on the density of the three-dimensional network in the gels. Because **3c** is more ionic than **3e**, the gel strength is more likely to be influenced by ionic strength. It is assumed that the high ionicity of the **3c** molecule leads to a closely packed three-dimensional network in the presence of ions.

The physical properties of supramolecular hydrogels were evaluated further on the basis of their thermal stability. Figure 6 shows the thermal stabilities for pure water gels

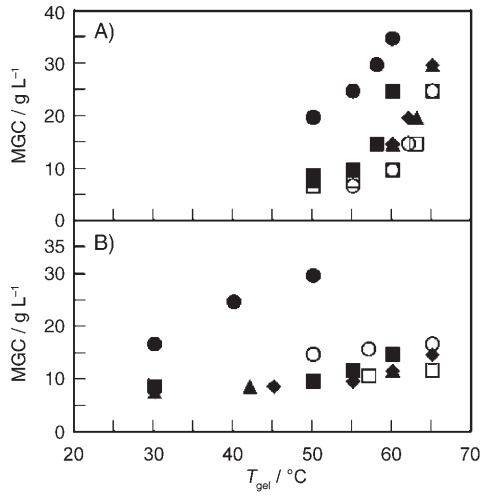

Figure 6. Thermal stabilities of A) pure water gels and B) saline gels based on **3b** (●), **3c** (■), **3d** (▲), **3e** (◆), **2e** (○), and **4e** (□).

(A) and saline gels (B) based on **3b** (●), **3c** (■), **3d** (▲), **3e** (◆), **2e** (○), and **4e** (□), and their sol–gel transition temperatures (T_{gel}) are listed in Table 4. The MGC values of pure water gels did not change between 25 and 50 °C, and they then increased with temperature. Above 65 °C, these hydrogelators cannot form a hydrogel, at even 80 $g L^{-1}$. On the other hand, although these gelators did not form a saline gel above 65 °C, the MGC values of saline gels exhibited little

Table 4. Physical data of pure water gels and saline gels of **2e**, **3b**–**3e**, and **4e**.[a]

	Pure water gel			Saline gel		
	strength [kPa]	T_{gel} [°C]	ΔH_{gel} [kJ mol^{-1}]	strength [kPa]	T_{gel} [°C]	ΔH_{gel} [kJ mol^{-1}]
3b	7.6	50	61	13.2	35	30
3c	7.2	55	163	12.4	65	36
3d	6.6	60	127	6.8	65	37
3e	6.1	60	130	6.5	65	37
2e	6.3	60	171	6.7	65	11
4e	6.2	60	168	6.3	65	11

[a] [Gelator] = 20 $g L^{-1}$ for gel strength and sol–gel transition temperature (T_{gel}).

change on increasing the temperature to 65 °C. These saline gels had higher T_{gel} values at the lower concentration than those of pure water gels (Table 4). To elucidate the thermal behavior, a thermodynamic analysis of the sol–gel transition was carried out by using van 't Hoff relationships.[26] From the relationship between MGC and T_{gel}, the sol–gel transition enthalpy (ΔH_{gel}) was determined from the slope of ln [gelator (mol L^{-1})] versus $1/T_{gel}$.[20] Surprisingly, the ΔH_{gel} values of the saline gels were much lower than those of pure water gels, although the saline gels showed high T_{gel} values at low concentrations. These results indicate that the saline gels are more thermally stable and their sol–gel transition energies are less than those of pure water gels. We have reported that the L-lysine hydrogelator with a sugar (non-ionic hydrogelator) forms a supramolecular hydrogel with high T_{gel} and ΔH_{gel} values in the presence of ions because the hydrophobic interaction becomes stronger.[19] In the present systems, the ionic interaction between carboxylate, alkali metal, proton, and carboxylic acid, in addition to hydrophobic and hydrogen-bonding interactions, play an important role in self-assembly into nanofibers (hydrogelation); namely, if the ionic interaction is absent, it is impossible to self-assemble into nanofibers (alternatively, micelles will form). The high ionic strength in the saline gel increases the intermolecular hydrophobic interaction and the thermal stability increases, which gives a high T_{gel} value. In the presence of many ions, the ionic interaction deceases and exchange between bulk cations and gelator cations is promoted. Presumably, the ionic interaction is destroyed by the attack of bulk ions, meanwhile the nanofibers are broken (collapse of the hydrogel), which results in the low ΔH_{gel} value for the sol–gel transition. The sol–gel transition of pure water gels occurs through almost simultaneous destruction of hydrophobic, hydrogen bonding, and ionic interactions (high T_{gel} and ΔH) by a thermal effect, whereas it occurs through destruction of hydrophobic and hydrogen-bonding interactions induced by breaking ionic interactions. The ΔH_{gel} values of the saline gels are therefore low compared with those of pure water gels.

Turbidity during the sol–gel transition: During the sol–gel transition experiments, the solutions exhibited interesting behavior. It is generally known that the dissolution of gelators by heating produces a clear solution.[1–2,4–5] In the present systems, clear solutions could not be obtained for **3d**, **3e**, **2e**, and **4e**, even on heating at 100 °C for more than 10 min. As shown in Figure 7, the hot opaque solution of **3e** (80 °C) changes to a translucent hydrogel (25 °C) during cooling. This behavior is thermally reversible. The behavior was studied by UV-visible spectroscopy. The transmittance at 600 nm was more than 80 % up to 70 °C and less than 0.4 % above 70 °C. From 25 °C to 65 °C, **3e** forms a translucent hydrogel and produces an opaque milky solution above 70 °C. These results indicate that hydrogelators form aggregates above 70 °C, which differs from the hydrogel.

Field emission scanning electron microscopy (FE-SEM) studies were carried out to elucidate the difference in nanostructures between hydrogels and opaque solutions. Figure 8 shows the FE-SEM images of samples of the opaque solution (A), a solution that contains a translucent hydrogel (B and C), and an opaque solution and translucent hydrogel (D) of **3e** (as shown in Figure 7). Here, samples B and C were obtained from the interface between the gel and opaque solution. The FE-SEM image of the hydrogel showed the formation of three-dimensional networks of the self-assembled nanofibers of **3e** (Figure 8D). Interestingly, the FE-SEM image of the opaque solution was quite different, it contained spherical aggregates and their interconnections. These aggregates differ from the micelles, shown in Figure 2A, and resemble precipitates. This result indicates that **3e** forms some spherical aggregates, similar to a colloid, in the hot solution at 80 °C, and these colloids are dispersed in the milky solution. Similar SEM images were observed with two-phase samples during hydrogelation (Figure 7): nanofibers from the hydrogel phase and spherical aggregates from the opaque solution phase.[20] On the other hand, the SEM images of the interface between the opaque solution and the hydrogel showed a mixture of nanofibers and spherical aggregates (Figure 8B and C). It is clear that the spheri-

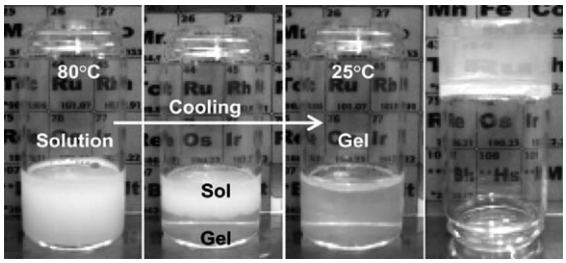

Figure 7. Hydrogelation process from an opaque solution to a translucent gel.

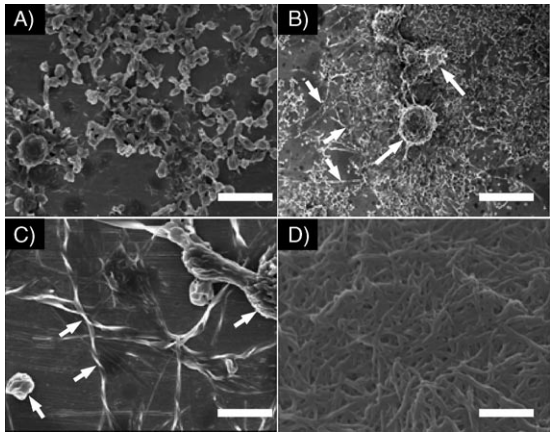

Figure 8. FE-SEM images of aggregates of **3e** (10 g L^{-1}). A) Samples prepared from an aqueous solution at 80 °C. B) and C) Samples of the interface between the gel and a solution of xerogel prepared from a solution containing translucent hydrogel and opaque solution at 50 °C. D) Xerogel prepared from translucent hydrogel (25 °C). All samples were prepared by freeze-drying. Scale bar: 200 nm (in A) and 500 nm (in B–D).

cal aggregates change to nanofibers during cooling, and this leads to hydrogelation.

Comparing the IR spectra of the hydrogel (25 °C) with that of the opaque solution (80 °C) shows that the absorbance at 1585 cm^{-1} decreases and the IR peak at 1726 cm^{-1} broadens into 1710 cm^{-1}.[20] This change is caused by breaking the interactions between the carboxylate, Na^+, H^+, and carboxylic acid; namely, **1** and **3** are separated. As mentioned above, because **1** does not dissolve in water unless it interacts with **3**, the opaque solution is a suspended precipitate of **1**. During cooling, compounds **1** and **3** again have ionic interactions, which leads to self-assembled nanofibers. Further experiments were carried out to confirm this mechanism. We first tried a dissolution test of **1** and **3**. Compound **3** was very soluble in water at room temperature, and **1** was insoluble in water, even on heating at 100 °C for 5 min. Addition of an equimolar quantity of **1** to the aqueous solution of **3**, and heating the solution to 90 °C, produced the opaque solution. The translucent hydrogel was then formed by cooling the hot opaque solution to 25 °C. This transition from a translucent hydrogel to an opaque solution is thermally reversible. This fact indicates that water-insoluble **1** dissolves in an aqueous solution in the presence of **3**. The next test was to identify the opaque solution. The hot opaque solution was filtered three times. The resulting white solid was washed with water and dried at 40 °C in a vacuum for 24 h. The ^1H NMR spectrum in $CDCl_3$ demonstrated that the white solid consisted of **1**. Therefore, the opaque milky solution obtained at 90 °C is a suspended precipitate of **1**. Note that the precipitate of **1** redissolves in water in the presence of **3** during cooling.

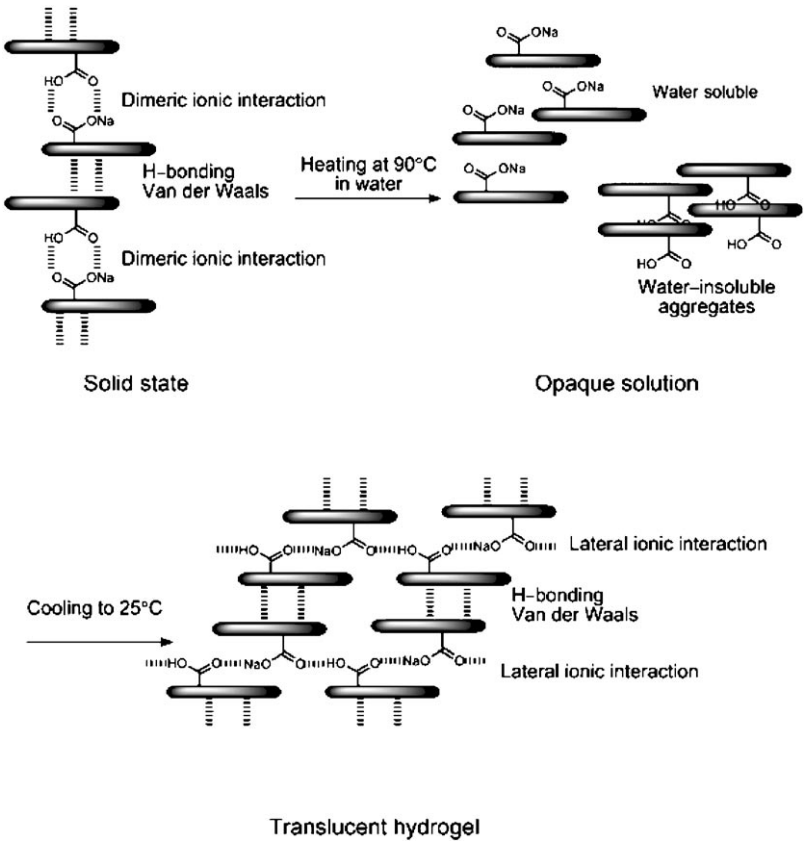

Scheme 1. Tentative illustration of hydrogelation mechanism of two-component hydrogelators.

Hydrogelation mechanism: These results enable us to propose a hydrogelation mechanism for the two-component systems (Scheme 1). In the solid state, compound **3e** has hydrogen-bonding and van der Waals interactions in addition to dimeric ionic interactions. On heating **3e** and water at 90 °C, compound **3e** dissolves in water and separates into **1** and **3**; this is followed by precipitation of **1** (to produce an opaque milky solution). During cooling, compound **1** redissolves in water by forming lateral ionic interactions with **3** to produce **3e**, which self-assembles into nanofibers through hydrogen-bonding and van der Waals interactions, thus leading to hydrogelation. The transition from an opaque solution to a translucent hydrogel is thermally reversible. Similarly, heating an aqueous solution of **3** and **1** to 90 °C produces an opaque solution, which forms a translucent hydrogel on cooling to 25 °C.

For pH-triggered hydrogelation, compounds **2** to **4** form a nanostructure of spherical micelles in water. The addition of aqueous HCl to the aqueous micelle solution with vigorous stirring results in partial protonation of the carboxylate groups, and the nanostructure changes to nanofibers. This creates a three-dimensional network, which results in hydrogelation.

Conclusion

In conclusion, we have shown that pH-triggered hydrogelation and amphiphilic gelation of two-component low-molecular-weight gelators that consist of a water-soluble alkali metal salt (**2**–**4**) and a water-insoluble carboxylic acid compound (**1**). The addition of aqueous HCl to aqueous solutions of **2** to **4** results in hydrogelation at room temperature. Partial protonation of the carboxylate to carboxylic acid induces lateral ionic interactions. Three-dimensional networks

are created by entanglement of nanofibers self-assembling through hydrogen-bonding and van der Waals interactions, which leads to the formation of supramolecular hydrogels. On the other hand, two-component low-molecular-weight gelators, which consist of **2** to **4** with **1**, functioned as amphiphilic gelators that were able to form not only hydrogels for pure water, saline, and aqueous solutions that contain inorganic salts, but also organogels for esters, ketones, cyclic ethers, aromatic solvents, and oils. At high temperatures (>70 °C), the two-component gelators produce a milky opaque aqueous solution that changes to a translucent hydrogel during cooling. Such behavior can be explained by the precipitation of **1**. The two-component gelators separate in the aqueous solution owing to thermal dissociation of ionic interactions, hydrogen bonds, and van der Waals interactions. The separated molecules of **1** form a spherical aggregate that involves their precipitation. During cooling to 25 °C, compound **1** dissolves in water as a result of ionic interactions with **3** to form a supramolecular hydrogel. Note that ionic interactions between **1** and **3** occur during cooling and **1** induces a thermally reversible precipitation–dissolution transition.

Experimental Section

Materials: N^{ε}-Lauroyl-L-lysine was kindly obtained from Ajinomoto. The other chemicals were of the highest grade commercially available and used without further purification. All solvents used in the syntheses were purified, dried, or freshly distilled, as required.

***N*$^{\alpha}$-Hexanoyl-*N*$^{\varepsilon}$-lauroyl-L-lysine (1)**: N^{ε}-Lauroyl-L-lysine (19.7 g, 60 mmol) was dissolved in water (500 mL) containing NaOH (12 g, 300 mmol), and ethyl ether (300 mL) was added. Hexanoyl chloride (13.5 g, 100 mmol) was added to the ether layer. The biphasic solution was vigorously stirred at 0 °C for 1 h and for a further 23 h at room temperature. The resulting solution was acidified with concentrated HCl (pH ≈1). The white precipitate was filtered, washed with water, and dried. The product was obtained by recrystallization (×2) from ethanol/ethyl ether (85 %). ^{1}H NMR (400 MHz, $CDCl_3$, TMS, 25 °C): δ = 0.86–0.90 (m, 6H; CH_3), 2.18 (t, J = 7.3 Hz, 2H; CH_2CONH), 2.24 (t, J = 7.0 Hz, 2H; NHCOCH_2), 3.19–3.26 (m, 2H; NHCH_2), 4.42–4.47 (m, 1H; CHNH), 6.30 (t, J = 5.6 Hz, 1H; N$^{\alpha}H$CO), 6.85 (d, J = 7.3 Hz, 1H; CON$^{\varepsilon}H$), 9.37 ppm (brs, 1H; COOH); IR (KBr): $\tilde{\nu}$ = 3311 (ν_{N-H}, amide A), 1733 ($\nu_{C=O}$, -COOH), 1638 ($\nu_{C=O}$, amide I), 1555 cm^{-1} (ν_{N-H}, amide II); elemental analysis calcd (%) for $C_{24}H_{46}N_2O_4$: C 67.57, H 10.87, N 6.57; found: C 67.88, H 10.99, N 6.58.

***N*$^{\alpha}$-Hexanoyl-*N*$^{\varepsilon}$-lauroyl-L-lysine lithium salt (2)**: A 4 M aqueous solution of LiOH (5 mL) was added to a stirred solution of **1** (8.5 g, 20 mmol) in ethanol (500 mL). Stirring was continued for 30 min, and the resulting solution was evaporated to dryness. The product was obtained by recrystallization from ethanol/ether (99 %). ^{1}H NMR (400 MHz, $CDCl_3$/[D_6]DMSO/TMS, 25 °C): δ = 0.86–0.90 (m, 6H; CH_3), 2.10–2.17 (m, 4H; NHCOCH_2), 3.05–3.13 (m, 2H; NHCH_2), 4.20 (q, J = 5.1 Hz, 1H; CH), 7.27 (d, J = 7.1 Hz, 1H; N$^{\varepsilon}H$), 7.39 ppm (t, J = 5.3 Hz, 1H; N$^{\alpha}H$); IR (KBr): $\tilde{\nu}$ = 3312 (ν_{N-H}, amide A), 1640 ($\nu_{C=O}$, amide I), 1597 (δ_{C-O}, COO$^-$), 1551 cm^{-1} (δ_{N-H}, amide II); elemental analysis calcd (%) for $C_{24}H_{45}N_2O_4Li$: C 66.64, H 10.49, N 6.48; found: C 66.68, H 11.03, N 6.51.

***N*$^{\alpha}$-Hexanoyl-*N*$^{\varepsilon}$-lauroyl-L-lysine sodium salt (3)**: The product was obtained by the same procedure as **2** with a 4 M aqueous solution of NaOH (5 mL) (99 %). ^{1}H NMR (400 MHz, $CDCl_3$, TMS, 25 °C): δ = 0.88 (t, J = 6.7 Hz, 6H; CH_3), 2.16 (t, J = 7.7 Hz, 4H; NHCOCH_2), 3.11 (brs, 2H; NHCH_2), 4.07 (brs, 1H; CH), 6.96 (brs, 1H; N$^{\varepsilon}H$), 7.47 ppm (brs, 1H; N$^{\alpha}H$); IR (KBr): $\tilde{\nu}$ = 3302 (ν_{N-H}, amide A), 1642 ($\nu_{C=O}$, amide I), 1592 (δ_{C-O}, COO$^-$), 1556 cm^{-1} (δ_{N-H}, amide II); elemental analysis calcd (%) for $C_{24}H_{45}N_2O_4Na$: C 64.25, H 10.11, N 6.24; found: C 64.31, H 10.34, N 6.26.

***N*$^{\alpha}$-Hexanoyl-*N*$^{\varepsilon}$-lauroyl-L-lysine potassium salt (4)**: The product was obtained by the same procedure as **2** with a 4 M aqueous solution of KOH (5 mL, 99 %). ^{1}H NMR (400 MHz, $CDCl_3$/[D_6]DMSO = 8:2, TMS, 25 °C): δ = 0.86–0.90 (m, 6H; CH_3), 2.12–2.20 (m, 4H; NHCOCH_2), 3.07–3.18 (m, 2H; NHCH_2), 4.02 (q, J = 5.1 Hz, 1H; CH), 7.28 (t, J = 5.3 Hz, 1H; N$^{\varepsilon}H$), 7.34 ppm (d, J = 7.1 Hz, 1H; N$^{\alpha}H$); IR (KBr): $\tilde{\nu}$ = 3301 cm^{-1} (ν_{N-H}, amide A), 1643 ($\nu_{C=O}$, amide I), 1590 (δ_{C-O}, COO$^-$), 1555 cm^{-1} (δ_{N-H}, amide II); elemental analysis calcd (%) for $C_{24}H_{45}N_2O_4K$: C 62.03, H 9.76, N 6.03; found: C 62.11, H 10.04, N 6.06.

***N*$^{\alpha}$-Hexanoyl-*N*$^{\varepsilon}$-lauroyl-L-lysine and its sodium salt (3a; 1/2 = 1:9)**: A 1 M aqueous solution of NaOH (18 mL) was added to a stirred solution of **1** (8.5 g, 20 mmol) in methanol (500 mL). Stirring was continued for 30 min, and the resulting solution was evaporated to dryness. The product was obtained by recrystallization from methanol/ether (99 %). ^{1}H NMR (400 MHz, $CDCl_3$, TMS, 25 °C): δ = 0.86–0.90 (m, 6H; CH_3), 2.18 (t, J = 7.7 Hz, 4H; CH_2CON$^{\varepsilon}$H), 2.25 (t, J = 7.7 Hz, 4H; N$^{\alpha}$HCOCH_2), 3.15–3.32 (m, 2H; N$^{\varepsilon}$HCH_2), 4.49 (q, J = 6.7 Hz, 1H; CHN$^{\alpha}$H), 6.17 (t, J = 5.6 Hz, 1H; N$^{\alpha}H$), 6.86 (d, J = 7.3 Hz, 1H; N$^{\varepsilon}H$), 10.55 ppm (brs, 1H; COOH); IR (KBr): $\tilde{\nu}$ = 3310 (ν_{N-H}, amide A), 1734 ($\nu_{C=O}$, -COOH), 1639 ($\nu_{C=O}$, amide I), 1553 cm^{-1} (δ_{N-H}, amide II); elemental analysis calcd (%) for $(C_{24}H_{46}N_2O_4)_{0.1}(C_{24}H_{45}N_2O_4Na)_{0.9}$: C 67.21, H 10.88, N 6.54; found: C 67.57, H 11.01, N 6.54.

***N*$^{\alpha}$-Hexanoyl-*N*$^{\varepsilon}$-lauroyl-L-lysine and its sodium salt (3b; 1/2 = 2:8)**: The product was obtained by the same procedure as **3** with a 1 M aqueous solution of NaOH (16 mL, 99 %). ^{1}H NMR (400 MHz, $CDCl_3$, TMS, 25 °C): δ = 0.86–0.90 (m, 6H; CH_3), 2.17 (t, J = 7.7 Hz, 4H; CH_2CON$^{\varepsilon}$H), 2.23 (t, J = 7.6 Hz, 4H; N$^{\alpha}$HCOCH_2), 3.16–3.23 (m, 2H; N$^{\varepsilon}$HCH_2), 4.41 (q, J = 6.6 Hz, 1H; CHN$^{\alpha}$H), 6.34 (brs, 1H; N$^{\alpha}H$), 6.96 ppm (brs, 1H; N$^{\varepsilon}H$), 10.18 (brs, 1H; COOH); IR (KBr): $\tilde{\nu}$ = 3309 cm^{-1} (ν_{N-H}, amide A), 1732 ($\nu_{C=O}$, -COOH), 1642 ($\nu_{C=O}$, amide I), 1549 cm^{-1} (δ_{N-H}, amide II); elemental analysis calcd (%) for $(C_{24}H_{46}N_2O_4)_{0.2}(C_{24}H_{45}N_2O_4Na)_{0.8}$ (444.21): C 66.91, H 10.72, N 6.50; found: C 67.00, H 10.88, N 6.50.

***N*$^{\alpha}$-Hexanoyl-*N*$^{\varepsilon}$-lauroyl-L-lysine and its sodium salt (3c; 1/2 = 3:7)**: The product was obtained by the same procedure as **3** with a 1 M aqueous solution of NaOH (14 mL) (99 %). ^{1}H NMR (400 MHz, $CDCl_3$, TMS, 25 °C): δ = 0.86–0.90 (m, 6H; CH_3), 2.15–2.24 (m, 4H; CH_2CON$^{\varepsilon}$H, N$^{\alpha}$HCOCH_2), 3.19 (q, J = 6.6 Hz, 2H; N$^{\varepsilon}$HCH_2), 4.37 (q, J = 6.7 Hz, 1H; CHN$^{\alpha}$H), 6.47 (brs, 1H; N$^{\alpha}H$), 7.06 (brs, 1H; N$^{\varepsilon}H$), 10.12 ppm (brs, 1H; COOH); IR (KBr): $\tilde{\nu}$ = 3306 (ν_{N-H}, amide A), 1727 ($\nu_{C=O}$, -COOH), 1643 ($\nu_{C=O}$, amide I), 1547 cm^{-1} (δ_{N-H}, amide II); elemental analysis calcd (%) for $(C_{24}H_{46}N_2O_4)_{0.3}(C_{24}H_{45}N_2O_4Na)_{0.7}$: C 66.57, H 10.64, N 6.47; found: C 66.63, H 10.91, N 6.47.

***N*$^{\alpha}$-Hexanoyl-*N*$^{\varepsilon}$-lauroyl-L-lysine and its sodium salt (3d; 1/2 = 4:6)**: The product was obtained by the same procedure as **3** with a 1 M aqueous solution of NaOH (12 mL) (99 %). ^{1}H NMR (400 MHz, $CDCl_3$, TMS, 25 °C): δ = 0.86–0.90 (m, 6H; CH_3), 2.15–2.23 (m, 4H; CH_2CON$^{\varepsilon}$H, N$^{\alpha}$HCOCH_2), 3.18 (brs, 2H; N$^{\varepsilon}$HCH_2), 4.34 (brs, 1H; CHN$^{\alpha}$H), 6.56 (brs, 1H; N$^{\alpha}H$), 7.11 (brs, 1H; N$^{\varepsilon}H$), 9.07 ppm (brs, 1H; COOH); IR (KBr): $\tilde{\nu}$ = 3305 (ν_{N-H}, amide A), 1725 ($\nu_{C=O}$, -COOH), 1643 ($\nu_{C=O}$, amide I), 1548 cm^{-1} (δ_{N-H}, amide II); elemental analysis calcd (%) for $(C_{24}H_{46}N_2O_4)_{0.4}(C_{24}H_{45}N_2O_4Na)_{0.6}$: C 66.24, H 10.57, N 6.44; found: C 66.30, H 10.84, N 6.44.

***N*$^{\alpha}$-Hexanoyl-*N*$^{\varepsilon}$-lauroyl-L-lysine and its sodium salt (3e; 1/2 = 5:5)**: The product was obtained by the same procedure as **3** with a 1 M aqueous solution of NaOH (10 mL) (99 %). ^{1}H NMR (400 MHz, $CDCl_3$, TMS, 25 °C): δ = 0.88 (t, J = 6.8 Hz, 6H; CH_3), 2.15–2.21 (m, 4H; CH_2CON$^{\varepsilon}$H, N$^{\alpha}$HCOCH_2), 3.16 (brs, 2H; N$^{\varepsilon}$HCH_2), 4.26 (brs, 1H; CHN$^{\alpha}$H), 6.70 (brs, 1H; N$^{\alpha}H$), 7.22 ppm (brs, 1H; N$^{\varepsilon}H$); IR (KBr): $\tilde{\nu}$ = 3306 (ν_{N-H}, amide A), 1710 ($\nu_{C=O}$, -COOH), 1643 ($\nu_{C=O}$, amide I), 1579 (δ_{C-O}, -COO$^-$), 1548 cm^{-1} (δ_{N-H}, amide II); elemental analysis calcd (%) for $(C_{24}H_{46}N_2O_4)_{0.5}(C_{24}H_{45}N_2O_4Na)_{0.5}$: C 65.91, H 10.49, N 6.41; found: C 65.99, H 10.77, N 6.41.

***N*$^{\alpha}$-Hexanoyl-*N*$^{\varepsilon}$-lauroyl-L-lysine and its sodium salt (3f; 1/2 = 6:4)**: The product was obtained by the same procedure as **3** with a 1 M aqueous solution of NaOH (8 mL) (99 %). ^{1}H NMR (400 MHz, $CDCl_3$, TMS, 25 °C):

$\delta = 0.88$ (t, $J = 6.9$ Hz, 6H; CH_3), 2.14–2.20 (m, 4H; $CH_2CON^{\varepsilon}H$, $N^{\alpha}HCOCH_2$), 3.15 (brs, 2H; $N^{\varepsilon}HCH_2$), 4.23 (brs, 1H; $CHN^{\alpha}H$), 6.72 (brs, 1H; $N^{\alpha}H$), 7.23 ppm (brs, 1H; $N^{\varepsilon}H$); IR (KBr): $\tilde{\nu} = 3305$ (ν_{N-H}, amide A), 1708 ($\nu_{C=O}$, -COOH), 1643 ($\nu_{C=O}$, amide I), 1595 cm^{-1} (δ_{C-O}, $-COO^-$), 1550 cm^{-1} (δ_{N-H}, amide II); elemental analysis calcd (%) for $(C_{24}H_{46}N_2O_4)_{0.6}(C_{24}H_{45}N_2O_4Na)_{0.4}$: C 65.58, H 10.41, N 6.37; found: C 65.67, H 10.66, N 6.37.

N^{α}-Hexanoyl-N^{ε}-lauroyl-L-lysine and its sodium salt (3g; 1/2 = 7:3): The product was obtained by the same procedure as **3** with a 1 M aqueous solution of NaOH (6 mL) (99%). ^{1}H NMR (400 MHz, $CDCl_3$, TMS, 25 °C): $\delta = 0.88$ (t, $J = 6.8$ Hz, 6H; CH_3), 2.14–2.20 (m, 4H; $CH_2CON^{\varepsilon}H$, $N^{\alpha}HCOCH_2$), 3.15 (brs, 2H; $N^{\varepsilon}HCH_2$), 4.21 (brs, 1H; $CHN^{\alpha}H$), 6.78 (brs, 1H; $N^{\alpha}H$), 7.28 ppm (brs, 1H; $N^{\varepsilon}H$); IR (KBr): $\tilde{\nu} = 3304$ (ν_{N-H}, amide A), 1708 ($\nu_{C=O}$, COOH), 1643 ($\nu_{C=O}$, amide I), 1596 (δ_{C-O}, $-COO^-$), 1550 cm^{-1} (δ_{N-H}, amide II); elemental analysis calcd (%) for $(C_{24}H_{46}N_2O_4)_{0.7}(C_{24}H_{45}N_2O_4Na)_{0.3}$: C 65.25, H 10.34, N 6.34; found: C 65.29, H 10.55, N 6.34.

N^{α}-Hexanoyl-N^{ε}-lauroyl-L-lysine and its sodium salt (3h; 1/2 = 8:2): The product was obtained by the same procedure as **3** with a 1 M aqueous solution of NaOH (4 mL) (99%). ^{1}H NMR (400 MHz, $CDCl_3$, TMS, 25 °C): $\delta = 0.88$ (t, $J = 6.8$ Hz, 6H; CH_3), 2.12–2.23 (m, 4H; $CH_2CON^{\varepsilon}H$, $N^{\alpha}HCOCH_2$), 3.13 (brs, 2H; $N^{\varepsilon}HCH_2$), 4.16 (brs, 1H; $CHN^{\alpha}H$), 6.85 (brs, 1H; $N^{\alpha}H$), 7.34 ppm (brs, 1H; $N^{\varepsilon}H$); IR (KBr): $\tilde{\nu} = 3305$ (ν_{N-H}, amide A), 1643 ($\nu_{C=O}$, amide I), 1597 (δ_{C-O}, $-COO^-$), 1551 cm^{-1} (δ_{N-H}, amide II); elemental analysis calcd (%) for $(C_{24}H_{46}N_2O_4)_{0.8}$-$(C_{24}H_{45}N_2O_4Na)_{0.2}$: C 64.91, H 10.26, N 6.31; found: C 64.99, H 10.34, N 6.31.

N^{α}-Hexanoyl-N^{ε}-lauroyl-L-lysine and its sodium salt (3i; 1/2 = 9:1): The product was obtained by the same procedure as **3** with a 1 M aqueous solution of NaOH (2 mL) (99%). ^{1}H NMR (400 MHz, $CDCl_3$, TMS, 25 °C): $\delta = 0.88$ (t, $J = 6.8$ Hz, 6H; CH_3), 2.16 (t, $J = 7.7$ Hz, 4H; $CH_2CON^{\varepsilon}H$, $N^{\alpha}HCOCH_2$), 3.13 (brs, 2H; $N^{\varepsilon}HCH_2$), 4.10 (brs, 1H; $CHN^{\alpha}H$), 6.88 (brs, 1H; $N^{\alpha}H$), 7.40 ppm (brs, 1H; $N^{\varepsilon}H$); IR (KBr): $\tilde{\nu} = 3305$ (ν_{N-H}, amide A), 1643 ($\nu_{C=O}$, amide I), 1597 (δ_{C-O}, $-COO^-$), 1553 cm^{-1} (δ_{N-H}, amide II); elemental analysis calcd (%) for $(C_{24}H_{46}N_2O_4)_{0.9}$-$(C_{24}H_{45}N_2O_4Na)_{0.1}$: C 64.85, H 10.19, N 6.27; found: C 64.92, H 10.29, N 6.27.

N^{α}-Hexanoyl-N^{ε}-lauroyl-L-lysine and its lithium salt (2e; H/Li = 5:5): The product was obtained by the same procedure as **3** with a 1 M aqueous solution of LiOH (10 mL) (99%). ^{1}H NMR (400 MHz, [D_6]DMSO, TMS, 25 °C): $\delta = 0.86$–0.90 (m, 6H; CH_3), 2.13 (t, $J = 7.6$ Hz, 4H; $CH_2CON^{\varepsilon}H$, $N^{\alpha}HCOCH_2$), 3.13 (q, $J = 6.1$ Hz, 2H; $N^{\varepsilon}HCH_2$), 4.32 (q, $J = 5.1$ Hz, 1H; $CHN^{\alpha}H$), 7.12 (t, $J = 5.6$ Hz, 1H; $N^{\alpha}H$), 7.20 ppm (d, $J = 7.3$ Hz, 1H; $N^{\varepsilon}H$); IR (KBr): $\tilde{\nu} = 3313$ (ν_{N-H}, amide A), 1734 ($\nu_{C=O}$, -COOH), 1641 ($\nu_{C=O}$, amide I), 1600 (δ_{C-O}, $-COO^-$), 1552 cm^{-1} (δ_{N-H}, amide II); elemental analysis calcd (%) for $(C_{24}H_{46}N_2O_4)_{0.5}(C_{24}H_{45}N_2O_4Li)_{0.5}$: C 67.11, H 10.68, N 6.53; found: C 67.21, H 10.77, N 6.53.

N^{α}-Hexanoyl-N^{ε}-lauroyl-L-lysine and its lithium salt (4e; H/K = 5:5): The product was obtained by the same procedure as **3** with a 1 M aqueous solution of KOH (10 mL) (99%). ^{1}H NMR (400 MHz, $CDCl_3$, TMS, 25 °C): $\delta = 0.86$–0.90 (m, 6H; CH_3), 2.19 (t, $J = 7.7$ Hz, 4H; $CH_2CON^{\varepsilon}H$, $N^{\alpha}HCOCH_2$), 3.12–3.18 (m, 2H; $N^{\varepsilon}HCH_2$), 4.25 (q, $J = 6.7$ Hz, 1H; $CHN^{\alpha}H$), 6.99 (t, $J = 5.5$ Hz, 1H; $N^{\alpha}H$), 7.13 ppm (d, $J = 7.3$ Hz, 1H; $N^{\varepsilon}H$); IR (KBr): $\tilde{\nu} = 3306$ (ν_{N-H}, amide A), 1704 ($\nu_{C=O}$, -COOH), 1643 ($\nu_{C=O}$, amide I), 1596 (δ_{C-O}, $-COO^-$), 1550 cm^{-1} (δ_{N-H}, amide II); elemental analysis calcd (%) for $(C_{24}H_{46}N_2O_4)_{0.5}(C_{24}H_{45}N_2O_4K)_{0.5}$: C 64.80, H 10.32, N 6.30; found: C 64.90, H 10.66, N 6.30.

Apparatus for measurements: The elemental analyses were performed with a Perkin–Elmer series II CHNS/O analyzer 2400. The variable temperature IR (VT-IR) spectra were recorded by using a JASCO FS-420 spectrometer. The TEM observations were carried out with a JEOL JEM-2010 electron microscope at 200 kV. The FE-SEM observation was carried out with a Hitachi S-5000 field emission scanning electron microscope. The ^{1}H NMR spectra were measured with a Bruker AVANCE 400 spectrometer with TMS as the standard. The UV/Vis spectra were measured with a JASCO V-570 UV/Vis/NIR spectrophotometer with a temperature controller (JASCO ETC-505T). The gel strengths were measured with a Sun Science Sun Rheo Meter CR-500DX.

pH-Triggered hydrogelation: A specific amount of 0.1 M aqueous HCl was added to an aqueous solution of **3** (20 mg) at 70 °C with stirring. The resulting solution was allowed to stand at 25 °C for 6 h. The reaction conditions are listed in Table 1.

Gelation test: A weighed gelator in solvent (1 mL) was heated in a sealed test tube until the gelator dissolved. After allowing the solution to stand at 25 °C for 6 h, its was evaluated by the "test-tube inversion" method.

Transmission electron microscope (TEM): Samples of hydrogels were prepared as follows: an aqueous solution of the gelator was dropped on a collodion- and carbon-coated 400 mesh grid, and the grid was quickly frozen in a liquid nitrogen. The frozen sample was dried in a vacuum for 24 h. The dried sample was negatively stained by osmic acid overnight, and then dried under reduced pressure for 2 h just before the measurement. Samples of organogels were prepared as follows: the gelator in benzene, 1,4-dioxane, or tetrachloromethane was dropped on a collodion- and carbon-coated 400 mesh grid and quickly dried in a vacuum for 24 h. After negative staining by osmic acid overnight, the grid was dried under reduced pressure for 2 h.

Field emission scanning electron microscopy (FE-SEM): Samples were prepared as follows: the aqueous solution of **3e** (10 $g L^{-1}$) in a capped test tube was heated at 80 °C for 5 min until the solution became opaque. The hot solution (80 °C), or the solution consisting of hydrogel and opaque solution (cooling to 50 °C), or the hydrogel (standing at 25 °C for 1 h) were quickly frozen in a dry ice/acetone bath (≈ -70 °C) for 20 min, and then freeze-dried with a vacuum pump for 24 h. These samples were sputtered with Pt-Pd.

Gel strength: Samples were prepared as follows: a mixture of a weighed gelator in water (2 mL) in a sealed vial (15 mm in diameter) was heated at 90 °C for 5 min. The resulting opaque solution was allowed to stand at 25 °C for 6 h. The gel strength was evaluated as the force required to sink a cylinder bar (10 mm in diameter) to a depth of 4 mm in the gel.

FTIR study: FTIR spectroscopy was performed in a spectroscopic cell with a CaF_2 window and 50 μm spacers operating at a 2 cm^{-1} resolution with 32 scans for solution and gel states and the KBr method for solid states.

VT-IR study: An automatic temperature-controlled cell unit (Specac Inc., P/N 20730) with a vacuum-tight liquid cell (Specac Inc., P/N 20502, path length 50 μm) fitted with CaF_2 windows was used to measure the IR spectra at different temperatures.

UV/Vis spectroscopy: UV/Vis spectra were measured as the transmittance at 600 nm in a spectroscopic quartz cell (path length 1 mm) after holding for 30 min at each temperature.

Acknowledgement

This study was supported by a Grant-in-Aid from The Global COE Program from the Ministry of Education, Culture, Sports, Science and Technology of Japan.

[1] a) *Molecular Gels: Materials with Self-Assembled Fibrillar Networks* (Eds.: P. Terech, R. G. Weiss), Springer, Dordrecht **2006**; b) *Top. Curr. Chem. Vol. 256: Low Molecular Mass Gelators: Design, Self-Assembly Function* (Ed.: F. Fages), Springer, Berlin, **2005**.

[2] a) Special issues: *Langmuir* **2002**, *18*, 7095–7173 and *Langmuir* **2002**, 19, 7174–7217; b) P. Terech, R. G. Weiss, *Chem. Rev.* **1997**, *97*, 3133–3159; c) D. J. Abdallah, R. G. Weiss, *Adv. Mater.* **2000**, *12*, 1237–1247; d) J. H. van Esch, B. L. Feringa, *Angew. Chem.* **2000**, *112*, 2351–2354; *Angew. Chem. Int. Ed.* **2000**, *39*, 2263–2266; e) L. A. Estroff, A. D. Hamilton, *Chem. Rev.* **2004**, *104*, 1201–1217; f) N. M. Sangeetha, M. Uday, *Chem. Soc. Rev.* **2005**, *34*, 821–836; g) M. de Loos, B. L. Feringa, J. H. van Esch, *Eur. J. Org. Chem.* **2005**, 3615–3631; h) M. George, R. G. Weiss, *Acc. Chem. Res.* **2006**,

39, 489–497; i) Low-molecular-weight organic gelators, D. K. Smith (Ed.), *Tetrahedron* **2007**, *63*, 7285–7494.

[3] a) *Supramolecular Polymers*, 2nd ed. (Ed.: A. Ciferri), CRC Press, Boca Raton, **1995**; b) T. Shimizu, *Polym. J.* **2003**, *35*, 1–22.

[4] a) M. Suzuki, Y. Nakajima, M. Yumoro, M. Kimura, H. Shirai, K. Hanabusa, *Org. Biomol. Chem.* **2004**, *2*, 1155–1159; b) D. R. Trivedi, A. Ballabh, P. Dastidar, B. Ganguly, *Chem. Eur. J.* **2004**, *10*, 5311–5322; c) A. R. Hirst, D. K. Smith, *Langmuir* **2004**, *20*, 10851–10857; d) S. J. Lee, S. S. Lee, J. S. Kim, J. Y. Lee, J. H. Jung, *Chem. Mater.* **2005**, *17*, 6517–6520; e) M. Takeuchi, S. Tanaka, S. Shinkai, *Chem. Commun.* **2005**, *5539*–5541; f) J.-L. Li, X.-Y. Liu, R.-Y. Wang, J.-Y. Xiong, *J. Phys. Chem. B* **2005**, *109*, 24231–24235; g) P. Terech, G. Clavier, H. Bouas-Laurent, J.-P. Desvergne, B. Demé, J.-L. Pozzo, *J. Colloid Interface Sci.* **2006**, *302*, 633–642; h) X. Huang, S. R. Raghavan, P. Terech, R. G. Weiss, *J. Am. Chem. Soc.* **2006**, *128*, 15341–15352; i) B.-Y. Wang, X.-Y. Liu, J. Narayanan, J.-Y. Xiong, J.-J. Li, *J. Phys. Chem. B* **2006**, *110*, 25797–25802; j) G. Zhu, J. S. Dordick, *Chem. Mater.* **2006**, *18*, 5988–5995; k) L. Su, C. Bao, R. Lu, Y. Chen, T. Xu, D. Song, C. Tan, T. Shi, Y. Zhao, *Org. Biomol. Chem.* **2006**, *4*, 2591–2594; l) M. George, S. L. Snyder, P. Terech, R. G. Weiss, *Langmuir* **2005**, *21*, 9970–9977; m) T. Pinaut, B. Isare, L. Bouteiller, *ChemPhysChem* **2006**, *7*, 816–819.

[5] a) M. Suzuki, M. Yumoto, M. Kimura, H. Shirai, K. Hanabusa, *Chem. Eur. J.* **2003**, *9*, 348–354; b) A. Heeres, C. van der Pol, M. Stuart, A. Friggeri, B. L. Feringa, J. van Esch, *J. Am. Chem. Soc.* **2003**, *125*, 14252–14253; c) L. A. Estroff, J. S. Huang, A. D. Hamilton, *Chem. Commun.* **2003**, *2958*–2959; d) S. M. Park, Y. S. Lee, B. H. Kim, *Chem. Commun.* **2003**, *2912*–2913; e) I. Yoshimura, Y. Miyahara, N. Kasagi, H. Yamane, A. Ojida, I. Hamachi, *J. Am. Chem. Soc.* **2004**, *126*, 12204–12205; f) D. K. Kumar, D. A. Jose, P. Dastidar, A. Das, *Langmuir* **2004**, *20*, 10413–10418; g) P. Terech, N. M. Sangeetha, B. Demé, U. Maitra, *J. Phys. Chem. B* **2005**, *109*, 12270–12276; h) J. H. Jung, Y. Do, Y.-A. Lee, T. Shimizu, *Chem. Eur. J.* **2005**, *11*, 5538–5544; i) A. Friggeri, C. van der Pol, K. J. C. van Bommel, A. Heeres, M. C. A. Stuart, B. L. Feringa, J. van Esch, *Chem. Eur. J.* **2005**, *11*, 5353–5361; j) Z. Yang, G. Liang, B. Xu, *Chem. Commun.* **2006**, *738*–740; k) P. Terech, N. M. Sangeetha, U. Maitra, *J. Phys. Chem. B* **2006**, *110*, 15224–15233; l) A. Mahler, M. Teches, M. Recher, S. Cohen, F. Gazit, *Adv. Mater.* **2006**, *18*, 1365–1370; m) Z. Yang, B. Xu, *Adv. Mater.* **2006**, *18*, 3043–3046.

[6] a) K. Hanabusa, T. Miki, Y. Taguchi, T. Koyama, H. Shirai, *J. Chem. Soc. Chem. Commun.* **1993**, *1382*–1383; b) X. Xu, M. Ayyagari, M. Tata, V. T. John, G. L. McPherson, *J. Phys. Chem.* **1993**, *97*, 11350-11353; c) K. Inoue, Y. Ono, Y. Kanekiyo, T. Ishii, K. Yoshihara, S. Shinkai, *J. Org. Chem.* **1999**, *64*, 2933–2937; d) M. de Loos, J. van Esch, R. M. Kellogg, B. L. Feringa, *Angew. Chem.* **2001**, *113*, 633–636; *Angew. Chem. Int. Ed.* **2001**, *40*, 613–616; e) B. A. Simmons, C. E. Taylor, F. A. Landis, V. T. John, G. L. McPherson, D. K. Schwartz, R. Moore, *J. Am. Chem. Soc.* **2001**, *123*, 2414–2421; f) S. Yangai, M. Higashi, T. Karatsu, A. Kitamura, *Chem. Mater.* **2004**, *16*, 3582–3585; g) A. Friggeri, O. Gronwald, K. J. C. van Bommel, S. Shinkai, D. N. Reinhoudt, *J. Am. Chem. Soc.* **2002**, *124*, 10754–10758; h) P. Babu, N. M. Sangeetha, P. Vijaykumar, U. Maitra, K. Rissanen, A. R. Raju, *Chem. Eur. J.* **2003**, *9*, 1922–1932; i) M. George, R. G. Weiss, *Langmuir* **2003**, *19*, 1017–1025; j) D. R. Trivedi, A. Ballabh, P. Dastidar, *Chem. Mater.* **2003**, *15*, 3971–3973; k) A. R. Hirst, D. K. Smith, M. C. Feiters, H. P. M. Geurts, *Langmuir* **2004**, *20*, 7070–7077; l) A. Ballabh, D. R. Trivedi, P. Dastidar, *Chem. Mater.* **2006**, *18*, 3795–3800; m) A. R. Hirst, D. K. Smith, *Chem. Eur. J.* **2006**, *12*, 5496–5508.

[7] a) M. Suzuki, Y. Sakakibara, S. Kobayashi, M. Kimura, H. Shirai, K. Hanabusa, *Polym. J.* **2002**, *34*, 474–477; b) G. Tan, M. Singh, J. He, V. T. John, G. K. McPherson, *Langmuir* **2005**, *21*, 9322–9326.

[8] a) Y. Ono, K. Nakashima, M. Sano, Y. Kanekiyo, K. Inoue, J. Hojo, S. Shinkai, *Chem. Commun.* **1998**, *1477*–1478; b) J. H. Jung, H. Kobayashi, M. Masuda, T. Shimizu, S. Shinkai, *J. Am. Chem. Soc.* **2001**, *123*, 8785–8789; c) S. Kobayashi, N. Hamasaki, M. Suzuki, M. Kimura, H. Shirai, K. Hanabusa, *J. Am. Chem. Soc.* **2002**, *124*, 6550–6551; d) S. Kawano, S. Tamaru, N. Fujita, S. Shinkai, *Chem. Eur. J.* **2004**, *10*, 343–351; e) P. Xue, R. Lu, Y. Huang, M. Jin, C. Tan, C. Bao, Z. Wang, Y. Zhao, *Langmuir* **2004**, *20*, 6470–6475; f) S. Che, A. Liu, T. Ohshima, K. Sakamoto, O. Terasaki, T. Tatsumi, *Nature* **2004**, *429*, 281–284; g) M. Suzuki, Y. Nakajima, T. Sato, H. Shirai, K. Hanabusa, *Chem. Commun.* **2006**, *377*–379; h) K. Hanabusa, T. Numazawa, S. Kobayashi, M. Suzuki, H. Shirai, *Macromol. Symp.* **2006**, *235*, 52–56; i) X. Huang, R. G. Weiss, *Langmuir* **2006**, *22*, 8542–8552; j) G. Roy, J. F. Miravet, B. Escuder, C. Sanchez, M. Llusar, *J. Mater. Chem.* **2006**, *16*, 1817–1824; k) Y. Zhou, Q. Ji, M. Masuda, S. Kamiya, T. Shimizu, *Chem. Mater.* **2006**, *18*, 403–406; l) Y. Yang, M. Suzuki, S. Owa, H. Shirai, K. Hanabusa, *J. Am. Chem. Soc.* **2007**, *129*, 581–587.

[9] a) M. Kimura, S. Kobayashi, T. Kuroda, K. Hanabusa, H. Shirai, *Adv. Mater.* **2004**, *16*, 335–339; b) P. Gao, C. Zhan, M. Liu, *Langmuir* **2006**, *22*, 775–779; c) P. Kumar, G. John, *Chem. Commun.* **2006**, *2218*–2220.

[10] J. D. Hartgerink, E. Beniash, S. I. Stupp, *Science* **2001**, *294*, 1684–1688.

[11] L. A. Estroff, L. Addadi, S. Weiner, A. D. Hamilton, *Org. Biomol. Chem.* **2004**, *2*, 137–141.

[12] a) K. Hanabusa, K. Hiratsuka, M. Kimura, H. Shirai, *Chem. Mater.* **1999**, *11*, 649–655; b) W. Kubo, T. Kitamura, K. Hanabusa, Y. Wada, S. Yanagida, *Chem. Commun.* **2002**, *374*–375; c) Y. Shibata, T. Kato, T. Kado, R. Shiratuchi, W. Takashima, K. Kaneto, S. Hayase, *Chem. Commun.* **2003**, *2730*–2731; d) N. Mohmeyer, P. Wang, H.-W. Schmidt, S. M. Zakeeruddin, M. Grätzel, *J. Mater. Chem.* **2004**, *14*, 1905–1909.

[13] a) T. Kato, *Science* **2002**, *295*, 2414–2418; b) M. P. B. van Bruggen, H. N. W. Lekkerkerker, *Langmuir* **2002**, *18*, 7141–7145; c) F. Camerel, C. F. J. Faul, *Chem. Commun.* **2003**, *1958*–1959; d) N. Mizoshita, Y. Suzuki, K. Hanabusa, T. Kato, *Adv. Mater.* **2005**, *17*, 692–696; e) X. Tang, Y. Zhao, B.-K. An, S. Y. Park, *Adv. Funct. Mater.* **2006**, *16*, 1799–1804.

[14] a) J. J. D. de Jong, L. N. Lucas, R. M. Kellogg, J. H. van Esch, B. L. Feringa, *Science*, **2004**, 304, 278–281; b) M. Ikeda, M. Takeuchi, S. Shinkai, *Chem. Commun.* **2003**, *1354*–1355; c) H. Koshima, W. Matsusaka, H. Yu, *J. Photochem. Photobiol. A* **2003**, *156*, 83–90; d) S. Y. Ryu, S. Kim, J. Seo, Y.-W. Kim, O.-H. Kwon, D.-J. Jang, S. Y. Park, *Chem. Commun.* **2004**, *70*–71; e) J. J. D. de Jong, L. N. Lucas, R. M. Kellogg, J. H. van Esch, B. L. Feringa, *Science* **2004**, *304*, 278–281; f) S. Yagai, T. Karatsu, A. Kitamura, *Langmuir* **2005**, *21*, 11048–11052; g) F. Würthner, B. Hanke, M. Lysetska, G. Lambright, G. S. Harms, *Org. Lett.* **2005**, *7*, 967–970; h) S. Miljanić, L. Frkanec, Z. Meić, M. Žinić, *Langmuir* **2005**, *21*, 2754–2760; i) X.-Q. Li, V. Stepanenko, Z. Chen, P. Prins, L. D. A. Siebbeles, F. Würthner, *Chem. Commun.* **2006**, *3871*–3873.

[15] S. Kiyonaka, S. Shinkai, I. Hamachi, *Chem. Eur. J.* **2003**, *9*, 976–983.

[16] a) J. C. Tiller, *Angew. Chem.* **2003**, *115*, 3180–3183; *Angew. Chem. Int. Ed.* **2003**, *42*, 3072–3075; b) B. Xing, C.-W. Yu, K.-H. Chow, P.-L. Ho, D. Fu, B. Xu, *J. Am. Chem. Soc.* **2002**, *124*, 14846–14847; c) L. Moreau, P. Barthélémy, M. El Maataoui, M. W. Grinstaff, *J. Am. Chem. Soc.* **2004**, *126*, 7533–7539.

[17] a) K. Sugiyasu, N. Fujita, M. Takeuchi, S. Yamada, S. Shinkai, *Org. Biomol. Chem.* **2003**, *1*, 895–899; b) O. Roubeau, A. Colin, V. Schmitt, R. Clérac, *Angew. Chem.* **2004**, *116*, 3345–3348; *Angew. Chem. Int. Ed.* **2004**, *43*, 3283–3286; c) T. Kitamura, S. Nakaso, N. Mizoshita, Y. Tochigi, T. Shimomura, M. Moriyama, K. Ito, T. Kato, *J. Am. Chem. Soc.* **2005**, *127*, 14769–14775; d) W. Weng, J. B. Beck, A. M. Jamieson, S. J. Rowan, *J. Am. Chem. Soc.* **2006**, *128*, 11663–11672; e) S. Bhuniya, B. H. Kim, *Chem. Commun.* **2006**, *1842*–1844.

[18] a) M. Suzuki, M. Yumoto, M. Kimura, H. Shirai, K. Hanabusa, *Helv. Chim. Acta* **2004**, *87*, 1–10; b) M. Suzuki, M. Nanbu, M. Yumoto, H. Shirai, K. Hanabusa, *New J. Chem.* **2005**, *29*, 1439–1444.

[19] M. Suzuki, S. Owa, H. Shirai, K. Hanabusa, *Tetrahedron* **2007**, *63*, 7302–7308.

[20] See the Supporting Information.

[21] K. L. A. Chan, S. G. Kazarian, *J. Comb. Chem.* **2006**, *8*, 26–31.

[22] Compounds **3f** to **3h** formed a D_2O gel at 20 g L^{-1}, but not **3i**, and **1** was water-insoluble. Because solutions and gels in D_2O contained

the insoluble compounds, their FTIR spectra in D_2O were not measured.
[23] Because the ratios of band areas around 1640 and 1560 cm^{-1} were below 10% against whole band area, these bands were ignored.
[24] Although **3a** and **3i** should have a cyclic dimer structure, it cannot be detected because of their low concentration. In addition, if these gelators do not have the cyclic dimer structure, the IR peak of carboxylic acid should be observed at 1730 cm^{-1}.
[25] N. Mohmeyer, H.-W. Schmidt, *Chem. Eur. J.* **2005**, *11*, 863–872.
[26] S. H. Seo, J. Y. Chang, *Chem. Mater.* **2005**, *17*, 3249–3254.

Received: July 19, 2007
Published online: December 27, 2007

